Molecular Neurobiology (2019) 56:5539–5554
https://doi.org/10.1007/s12035-019-1468-7

Nanocarrier-mediated Delivery of CORM-2 Enhances Anti-allodynic and Anti-hyperalgesic Effects of CORM-2

Hari Prasad Joshi[1] · Sung Bum Kim[2] · Seungki Kim[3] · Hemant Kumar[1] · Min-Jae Jo[1] · Hyemin Choi[1] · Juri Kim[1] · Jae Won Kyung[1] · Seil Sohn[1] · Kyoung-Tae Kim[4,5] · Jin-Ki Kim[6] · In-Bo Han[1]

Received: 6 July 2018 / Accepted: 4 January 2019 / Published online: 12 January 2019

Abstract

Neuropathic pain is a devastating chronic condition and effective treatments are still lacking. Carbon monoxide-releasing molecule-2 (CORM-2) as a carbon monoxide (CO) carrier, exerts potent anti-neuropathic pain effects; however, its poor water solubility and short half-life hinder its clinical utility. Therefore, the aim of this study was to investigate whether CORM-2-loaded solid lipid nanoparticles (CORM-2-SLNs) enhance the anti-allodynic and anti-hyperalgesic effects of CORM-2 in a rat chronic constriction injury (CCI) model. CORM-2-SLNs were prepared using a nanotemplate engineering technique with slight modifications. The physiochemical properties of CORM-2-SLNs were characterized and CO release from CORM-2-SLNs was assessed using a myoglobin assay. CO was slowly released from CORM-2-SLNs, was observed, and the half-life of CO release was 50 times longer than that of CORM-2. In vivo results demonstrate that intraperitoneal administration of CORM-2-SLNs (5 and 10 mg/kg/day, ip) once daily for seven consecutive days significantly reduced the mechanical allodynia and mechanical hyperalgesia compared with CORM-2 (10 mg/kg/day, ip). RT-PCR and Western blot analyses on days 7 and 14, revealed that treatment with CORM-2-SLNs resulted in greater reductions in the CCI-elevated levels of heme-oxygenase-2 (HO-2); inducible nitric oxide synthase (iNOS); neuronal NOS (nNOS); and inflammatory mediators (TNF-α, IBA-1, and GFAP) in the spinal cord and dorsal root ganglions compared with treatment with CORM-2. In contrast, HO-1 and IL-10 were significantly increased in the CORM-2-SLN-treated group compared with the group treated with CORM-2. These data indicate that CORM-2-SLNs are superior to CORM-2-S in alleviating mechanical allodynia and mechanical hyperalgesia.

Keywords Neuropathic pain · Nanoparticles · Allodynia · Hyperalgesia · Carbon monoxide releasing molecule · Carbon monoxide

Hari Prasad Joshi, Sung Bum Kim and Seungki Kim contributed equally to this work.

Electronic supplementary material The online version of this article (https://doi.org/10.1007/s12035-019-1468-7) contains supplementary material, which is available to authorized users.

✉ Jin-Ki Kim
jinkikim@hanyang.ac.kr

✉ In-Bo Han
hanib@cha.ac.kr

[1] Department of Neurosurgery, CHA Bundang Medical Center, School of Medicine, CHA University, 59 Yaptap-ro, Bundang-gu, Seongnam-si, Gyeonggi-do 13496, Republic of Korea

[2] Department of Neurosurgery, Kyung Hee University, Dongdaemun-gu, Seoul 02447, Republic of Korea

[3] Department of Surgery, CHA Bundang Medical Center, School of Medicine, CHA University, Seongnam-si, Gyeonggi-do 13496, Republic of Korea

[4] Department of Neurosurgery, School of Medicine, Kyungpook National University, Daegu, South Korea

[5] Department of Neurosurgery, Kyungpook National University Hospital, Daegu, South Korea

[6] College of Pharmacy and Institute of Pharmaceutical Science and Technology, Hanyang University, 55 Hanyangdeahak-ro, Sangnok-gu, Ansan, Gyeonggi-do 15588, Republic of Korea

Introduction

Neuropathic pain resulting from lesions or diseases of the somatosensory system remains an extremely important problem because currently available treatments have limited efficacy [1]. Neuropathic pain is characterized by exaggerated responses to normally painful stimuli (hyperalgesia), pain response to normally mild stimuli (allodynia), and spontaneous pain (pain that occurs without a trigger) [2].

The mechanisms of neuropathic pain are complex, not fully elucidated, and remain controversial [3, 4]. Because effective treatments are still lacking, researchers are constantly searching for new treatment solutions. Recent data have shed light on the biological function of carbon monoxide (CO)—a compound reported to confer tissue protection through anti-inflammatory, anti-proliferative, anti-oxidant, anti-apoptotic, and vasodilatory effects [5]. However, CO is considered a toxic gas and is commonly known as the "silent killer." CO primarily mediates its toxic effects in humans by strongly binding to hemoglobin leading to the formation of carboxyhemoglobin (COHb). In the presence of COHb, oxygen-bound hemoglobin levels are reduced, leading to decreased oxygen delivery to tissues and subsequent hypoxic tissue damage and death [6]. Interestingly, CO is endogenously generated as a degradation product of the heme oxygenase (HO) pathway [7]. CO is considered to be an important and versatile mediator of physiological processes and previous studies have revealed that CO inhalation at a low concentration (50–500 ppm) has potent anti-inflammatory effects in several models of lung or vascular injury and ischemia–reperfusion injury [8, 9]. Although CO has a number of potential therapeutic benefits, its gaseous property limits its clinical utility; CO gas therapy requires continuous dose control and special hospital care [7, 10–12].

To limit direct inhalation requirements for the delivery of CO gas, carbon monoxide-releasing molecules (CORMs) have been developed as a means of administering CO in a controlled manner [12]. CORMs are transition metal complexes capable of reproducing many biological effects of HO-1-derived CO. Several types of CORMs, including CORM-1 [$Mn_2(CO)_{10}$], CORM-2 [$(Ru(CO)_3Cl_2)_2$], CORM-3 [$Ru(CO)_3Cl$-glycinate], and CORM-A_1 [$Na_2(H_3BCO_2)$] have been investigated [13]. Among them, CORM-2 shows anti-inflammatory, anti-nociceptive, anti-allodynic, and anti-hyperalgesic effects; however, the half-life of CO is too short (~ 1 min) and CORM-2 has low hydrophilicity and high lipophilicity [10, 14]. To improve CORM-2 bioavailability by increasing dissolution rate, the use of controlled-release techniques to deliver CORM-2 could be an attractive strategy.

Solid lipid nanoparticles (SLNs) have been considered as an alternative drug carrier system with several advantages (e.g., enhanced physical stability, bioavailability, drug loading ability for lipophilic and hydrophilic drugs, low cost, and high feasibility for large-scale manufacturing) [15, 16] [17]. SLNs are nanosized colloidal drug delivery systems composed of a biodegradable solid lipid core and stabilizer [16, 18]. It is well-known that the release of incorporated drugs from SLNs could be controlled by using different types of lipids and surfactants [19–21]. In a previous study by this group, CORM-2-loaded lipid nanoparticles were formulated to improve the solubility of CORM-2 by incorporating CORM-2 in a solid lipid core allowing for the slow release of CO [22].

In the present study, we investigated whether CORM-2-SLNs could enhance the anti-allodynic and anti-hyperalgesic effects of CORM-2 in a rat chronic constriction injury (CCI) model. To confirm this, we compared CO release from CORM-2 solution (CORM-2-S) and CORM-2-SLNs using an in vitro myoglobin assay. Additionally, we compared the anti-allodynic and anti-hyperalgesic effects produced by intraperitoneal administration of CORM-2-S and CORM-2-SLNs in a rat CCI model. The effects of the treatments on the expression of HO-1, HO-2, inducible nitric oxide synthase (iNOS), neuronal NOS (nNOS), IL-10, and inflammatory mediators (TNF-α, ionized calcium-binding adapter molecule-1 (IBA-1), and glial fibrillary acidic protein (GFAP)) in the dorsal root ganglions (DRGs) and the dorsal horns of the L4–L6 spinal cord were also assessed.

Materials and Methods

Preparation of CORM-2-SLNs

CORM-2 was purchased from Sigma-Aldrich (St. Louis, MO, USA). CORM-2-SLNs were prepared by a nanotemplate engineering technique with slight modifications [23]. Briefly, the mixture of CORM-2, palmityl alcohol, Tween 40, Span 40, and Myri S40 (1.0:1.0:1.5:0.3:3.0, weight ratio) were mixed and melted in a water bath at 70 °C. Then, a preheated 5% dextrose solution for injection was added to the melted mixture. After stirring in a water bath at 70 °C for 50 min, clear nanoemulsions were cooled down at 4 °C, resulting in solid lipid nanoparticles. The prepared CORM-2-SLNs were filtered through a 0.2-μm polyvinyl difluoride (PVDF) syringe filter to remove unincorporated CORM-2 or large aggregates.

Physicochemical Characterization of CORM-2-SLNs

The average particle size and polydispersity index of CORM-2-SLNs were determined by photon correlation spectroscopy using a Zetasizer Nano ZS (Malvern, Worcestershire, UK). Prior to measurement, CORM-2-SLNs were diluted 100 times with filtered deionized water. The zeta potential of CORM-2-SLNs was measured by electrophoretic light scattering using the same instrument. The incorporation efficiency of CORM-

2-SLNs was determined by quantifying ruthenium in CORM-2 using inductively coupled plasma atomic emission spectrophotometry (ICP-AES). The filtered CORM-2-SLNs were analyzed for ruthenium contents by Spectro Arcos (Spectro, Kleve, Germany) with a detection wavelength at 240.3 nm. The incorporation efficiency of CORM-2-SLNs was calculated by using the following equation.

$$\text{Incorporation efficiency}\,(\%) = \frac{\text{Amount of ruthenium in CORM2-SLNs}}{\text{Total amount of ruthenium added}} \times 100 \quad (1)$$

CO Release from CORM-2-SLNs

CO release from the CORM-2-SLNs was determined by a myoglobin assay [22, 24]. The amount of carbonmonoxy-myoglobin (MbCO) formed from deoxy-myoglobin (deoxyMb) on CO release was quantified by measuring the absorbance at 510 and 540 nm by a UV-Vis spectrophotometer (Ultrospec 7000, Biochrom Ltd., Cambridge, UK). CORM-2-SLNs and the CORM-2 solution were added to 1 mL of deoxyMb solution to give 20 μM of CORM-2 concentration, respectively. Then, 500 μL of mineral oil was added to the top of the mixture to prevent CO escaping or the oxygenation of myoglobin. The concentration of MbCO was calculated at regular intervals until the plateaus were reached.

It has been reported that no elevation of basal HbCO levels at therapeutic doses after intraperitoneal and intravenous administration of CORM-2 was detected [7, 25]. In the current study, therefore, we mainly focused on in vitro CO release from CORM-2-SLNs and in vivo pharmacological effects against disease models.

Storage Stability of CORM-2-SLNs

The stability of CORM-2-SLNs was evaluated for 28 days after storage at 4 °C. The time-course changes in particle size, PDI, and zeta potential were measured by using a Zetasizer Nano ZS (Malvern, Worcestershire, UK) as describe above. In addition, CO release was compared with the freshly prepared CORM-2-SLNs by using a myoglobin assay to ensure the retention of CO releasing ability of CORM-2-SLNs.

Animals

All animal experiments were performed according to the approved protocol by the Institutional Animal Care and Use Committee (IACUC) of our institute (IACUC170005) and Guide for the Care and Use of Laboratory Animals (National Institutes of Health, Bethesda, MD, USA). Adult female Sprague-Dawley (SD) rats (2–3 months, 200–240 g) were purchased from Orient Bio Inc. (Seongnam, Gyeonggi-do, South Korea). Animals were kept in plastic cages with enough sawdust and maintained on a standard 12:12 h light/dark cycle at a room temperature of 23 ± 3 °C with food and water available ad libitum. Animals were acclimatized to the environment for at least 1 week prior to use in the experiments. Experiments were performed during the light cycle (always between 10 a.m. to 4 p.m.).

Induction of Neuropathic Pain

Surgeries were performed in sterile conditions. Rats were deeply anesthetized by intraperitoneal injection of tiletamine and zolepam (Zoletil® 50 mg/kg) and xylazine (Rompun® 10 mg/kg). Neuropathic pain was induced by chronic constriction injury (CCI) model [26]. Briefly, a blunt cut was made in the lateral surface of the left hind limb, and the biceps femoris was separated to expose the sciatic nerve. Four sterile loose ligatures (silk 4–0; AILEE Co., Ltd, Busan, South Korea) were tied around the proximal part of the trifurcation of the nerve with a distance of 1 mm between each ligature. After the nerve ligation, the wound was sutured. A sham operation was performed as described above except that the nerve was not ligated.

Drug Administration

Pregabalin (Lyrica®) was purchased from Pfizer (Sandwich, Kent, CT13 9NJ). It was dissolved in water and administered orally at dose 10 mg/kg po from the day of surgery to 1 week. [27]. CORM-2 solution (CORM-2-S) and CORM-2-SLNs (equivalent to 10 mg/kg of CORM-2) were freshly prepared before use and intraperitoneally administered at 10 mg/kg in a final volume of 850 μL, once per day from the day of surgery to 1 week. The control group received the same volume of 5% dextrose solution. The dose and duration of CORM-2-S and CORM-2-SLNs treatment was chosen based on a previous report [28]. In order to investigate the superiority of treatment with CORM-2-SLNs, we also compared low-dose CORM-2-SLNs (5 mg/kg, ip) with CORM-2-S (10 mg/kg, ip) in the same animal model.

We tried to dose the same amount of CORM-2 and quantified the amount of Ru using ICP-AES since it is more accurate way for evaluating the concentration of CORM-2. Therefore, the same amount of CORM-2 was contained in CORM-2 solution and CORM-2-SLNs.

Experimental Design

The whole experiment was divided into two parts: (a) 7-day animal experiment and (b) 14-day animal experiment. A total of nine animals per group were used for the 14-day

experiment in which behavior tests, PCR, and western blotting were performed. A total of six animals were used in each group for the 7-day experiment in which PCR and western blotting were performed. Behavior was performed in six experimental groups: naïve animals (healthy animals, no surgery, no injection); sham group (those ones underwent a similar surgery except sciatic nerves that were not ligated); injury group (CCI animals treated with at a dose of 10 mg/kg 5% dextrose, ip); pregabalin (PGB)-treated group [CCI animals treated with PGB (10 mg/kg/day, po)]; CORM-2-S-treated group [CCI animals treated with CORM-2-S (10 mg/kg, ip)]; and CORM-2-SLN-treated group [CCI animals treated with CORM-2-SLNs (5 and 10 mg/kg, ip)]. However, behavior data did not revealed significant difference between PGB and CORM-2-S, so PGB group was not used in biochemical studies. Animals were sacrificed at days 7 and 14 after injury and the ipsilateral DRGs and the dorsal horns of the L4–L6 spinal cords were removed, frozen, and preserved for RT-PCR and Western blot assay (Fig. 1).

Behavioral Test

Allodynia and hyperalgesia to mechanical and chemical stimulus were used as outcome measures of neuropathic pain. Behavior test was performed by two blinded evaluators. The testing environment was kept quiet and well controlled with constant temperature and humidity. Tests were carried out at a similar time of day.

Mechanical Allodynia

It was quantified by measuring the hind paw withdrawal response to von Frey filament stimulation. In brief, rats were placed individually in transparent Plexiglas® box and were arranged upon a perforated metal floor and acclimatized for 1 h. A dynamic plantar von Frey aesthesiometer (Ugo Basile, Italy) was used to measure the mechanical allodynia. The paw withdrawal threshold (PWT) value was recorded to measure mechanical allodynia. Behavior measurement was performed 1 day before CCI and at days 1, 3, 7, and 14 after CCI. However, assessing pain behavior at day 1 was practically strenuous, so we omitted day 1 after CCI in rest of the behavior experiments. The paw withdrawal threshold (g) was recorded from both injured and uninjured hind paws in a counterbalanced order. Clear paw withdrawal, licking, shaking, or sniffing denotes pain behavior. A positive response was defined as the PWT, when rats showed at least three withdrawal responses out of five times application to a filament and the mean value was used for statistical analysis (Supplementary data 1 and 2).

Cold Allodynia

The response to cold stimulation was assessed by spraying 50 μL of acetone onto the plantar surface of hind paw with the blunt needle connected to a syringe [29]. Paw withdrawal response was recorded at arbitrary minimal value of 0.5 s and cutoff value of 15 s.

Mechanical Hyperalgesia

Pinprick test was performed to assess mechanical hyperalgesia [30]. In which, the plantar surface of the hind paw was gently stimulated with the point of safety pin at an intensity that can produce a withdrawal response in normal animal preventing the skin penetration (pinprick test). Stop watch was used to

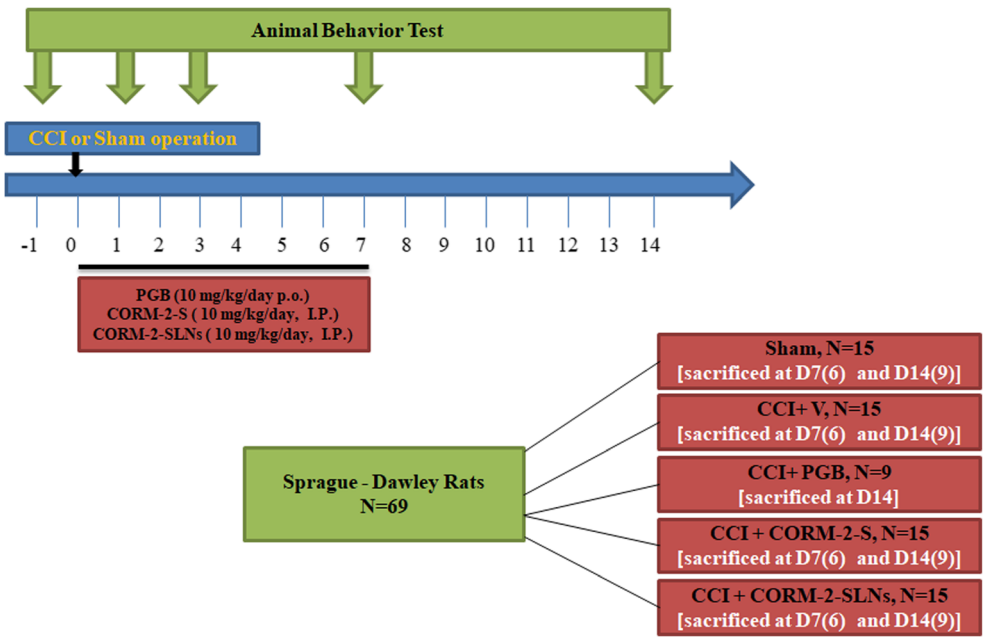

Fig. 1 Experimental design: showing total no. of animal used in this study, experimental groups, drug treatment with specified dose and time period, and behavior analysis assessed at different time period

record the paw withdrawal duration. It was set to an arbitrarily minimal time of 0.5 s (for the brief normal response) and cutoff time of 15 s.

Quantitative Real-Time Reverse Transcription Polymerase Chain Reaction (qRT-PCR)

Animals were rapidly sacrificed by CO_2 overdosing. The ipsilateral DRGs and the dorsal horns of the L4–L6 spinal cords were removed, and homogenized using T 25 digital homogenizer (IKA, Seoul, South Korea) in TRIzol reagent (Ambion, Carlsbad, CA) according to the manufacturer's instruction for RNA extraction. RNA quantity and purity were measured using a NanoReady (FC-1100, Hangzhau LifeReal Biotechnology, Hangzhou, China) (Nanoready Software, version 1.5.5). Complementary DNA was made from 1 μg of RNA using a Maxime RT PreMix kit (25081, Korea). Quantitative real-time PCR was performed using a SYBR Green Master Mix (21966100, Sigma-Aldrich, Germany), and the detection of mRNA was analyzed using an ABI Step One Real-time PCR System (Applied Biosystems, Foster City, CA, USA). The primers were purchased from Bioneer (Daejeon, Korea). The primer sequences used in this study are shown in Table 1.

The PCR amplifications were performed at 95 °C for 30 s, followed by 45 cycles of thermal cycling at 95 °C for 5 s, 56 °C for 30 s, and 72 °C for 30 s. Melt curves were performed on completion of the cycles to remove any non-specific product. Quantification was performed by normalizing the cycle threshold (Ct) values with β-actin and analyzed by the ΔΔCT. These experiments were repeated three times.

Table 1 Nucleotide sequences for our target gene and reference gene (β-actin)

Primers	Direction	Sequences
HO-1	Sense	5′-CGTGCAGAGAATTCTGAGTTC-3′
	Anti-sense	5′-AGACGCT TTACGTAGTGCTG-3′
IBA-1	Sense	5′-GCCTCATCGT CATCTCCCCA-3′
	Anti-sense	5′-AGGAAGTGCTTGTTGATCCCA-3′
TNF-α	Sense	5′-GTTCTATGGCCCAGACCCTCAC-3′
	Anti-sense	5′-GGC ACC ACTAGTTGGTTGTCTTTG-3′
nNOS	Sense	5′-TGGCAGCCCTAAGA CC TATG-3′
	Anti-sense	5′-AGTCCGAAAATGTCCTCGTG-3′
iNOS	Sense	5′-CATCGGCA GGATTCAGTGGT-3′
	Anti-sense	5′-GTGTGGTGGTCCATGATGGT-3′
IL-10	Sense	5′-CAGAGCCACATGCTCCTAGA-3′
	Anti-sense	5′-TGTCCAGCTGGTCCTTTGTT-3′
β-Actin	Sense	5′-CCAGAGCAAGAGAGGCATCCTG-3′
	Anti-sense	5′-GCCGATAGTGATGACCTGACCGT-3′

β-actin beta-actin, *HO-1* hemeoxygenase-1, *IBA-1* ionized calcium-binding adapter molecule-1, *TNF-α* tumor necrosis factor-alpha, *nNOS* neuronal nitric oxide synthase, *iNOS* inducible nitric oxide synthase, *IL-10* interleukin 10

Western Blot Analysis

At 7 and 14 days after surgery, ipsilateral DRGs and the dorsal horns of the L4–L6 spinal cords were frozen in liquid nitrogen and stored at − 80 °C until assay. Tissues were homogenized in ice-cold lysis buffer (PRO-PREP™, iNtRON biotechnology) and centrifuged at 4 °C for 15 min at 12,000*g*. The supernatant, consisting of 40 μg protein, was mixed with 5× Laemmli loading buffer (G031, abm, Canada) and then loaded onto 4% stacking/10% separating sodium dodecyl sulfate polyacrylamide gels, except for IBA-1 (15%). Proteins were electrophoretically transferred onto a polyvinylidene difluoride membrane (#162-0177, Bio-Rad, USA) for 2 h. After transfer, the membranes were blocked with PBST+ 5% nonfat dry milk and incubated overnight at 4 °C with anti-HO-1 (1:1000, Abcam, USA), anti-HO-2 (1:1000, Cell Signaling, USA), anti-nNOS (1:1000, Abcam), anti-iNOS (1:500, Abcam), anti-IBA-1(1:2000, Abcam), and anti-GFAP (1:20000, Abcam), anti-IL-10 (0.1 μg/ml, Abcam), and anti-TNF-α (1:1000, Abcam). The proteins were detected by a horseradish peroxidase-conjugated secondary antibody (Gene Tex, 2456 Alton Pkwy Irvine, CA 92606, USA) and visualized with chemiluminescence reagents (ECL kit; GE Healthcare, UK) using a photographic film detection instrument (LAS 400). The membranes were stripped and reprobed with a monoclonal rabbit anti-β-actin antibody (1:10000, Sigma, USA) used as a loading control. The intensity of blots was captured and quantified by ImageJ software.

Statistical Analysis

Data are expressed as the mean ± standard deviation. Behavioral data and western blot quantification data were analyzed by two-way ANOVA followed by Bonferroni's post hoc tests. The density of specific bands from western blotting was quantified by a computer-assisted imaging analysis system (ImageJ, NIH). The PCR data were analyzed by one-way ANOVA followed by Tukey's test to compare all pairs of the column. $P < 0.05$ was considered as statistically significant. All statistical analysis was performed by using GraphPad Prism 5 software (Inc., La Jolla, CA, USA).

Results

Preparation and Physicochemical Characterization of CORM-2-SLNs

CORM-2-SLNs were successfully prepared using a nanotemplate engineering technique with a solid lipid core

(palmityl alcohol) and a surfactant mixture (Tween 40, Span 40, and Myrj S40). The physicochemical properties of CORM-2-SLNs (i.e., particle size, polydispersity index, zeta potential, and incorporation efficiency) are presented in Table 2.

CORM-2-SLNs had a mean particle size of 119.5 ± 3.2 nm with narrow particle size distribution indicated by a polydispersity index below 0.150. The zeta potential of CORM-2-SLNs was − 4 mV. The amount of ruthenium in CORM-2-SLN was measured by ICP-AES, and the incorporation efficiency was calculated to be 94.0 ± 0.7%.

Although the structure of CORM-2 was not identified through nuclear magnetic resonance (NMR) and infrared (IR) spectroscopy after preparation of CORM-2-SNLs, the morphology of the nanoparticle was evaluated by transmission electron microscopy (TEM), and it was confirmed that spherical particles about 100 nm were produced. Hydrophobic CORM-2 was located in the lipid core of the SLN during the manufacturing process, and the non-loaded CORM-2 was removed through the filter. After the production of SLN, myoglobin analysis showed that CO was normally produced.

CO Release from CORM-2-SLNs

The concentration of MbCO was analyzed to determine the time-course release of CO from CORM-2-SLNs under physiological conditions. CORM-2-SLNs showed a slow CO release compared with CORM-2-S (Fig. 2a). An instantaneous release of CO from CORM-2-S was observed—more than 70% of CO was released within 1.5 min. In the case of CORM-2-SLNs, CO release was slower and retained until 60 min. To compare the initial CO release between CORM-2-SLNs and CORM-2-S, the CO release profiles within 5 min were analyzed more closely (Fig. 2b). Approximately 27% and 81% of CO was released from CORM-2-SLNs and CORM-2-S, respectively. Moreover, the CO release half-life of CORM-2-SLNs was 50 times longer than that of CORM-2-S (from 0.25 to 12.5 min).

Storage Stability of CORM-2-SLNs

To investigate the storage stability of CORM-2-SLNs, particle size, zeta potential, polydispersity index, and CO release were determined for 28 days after storage at 4 °C. As presented in Table 3, these parameters were not significantly changed for 28 days indicating that CORM-2-SLNs were stable at 4 °C.

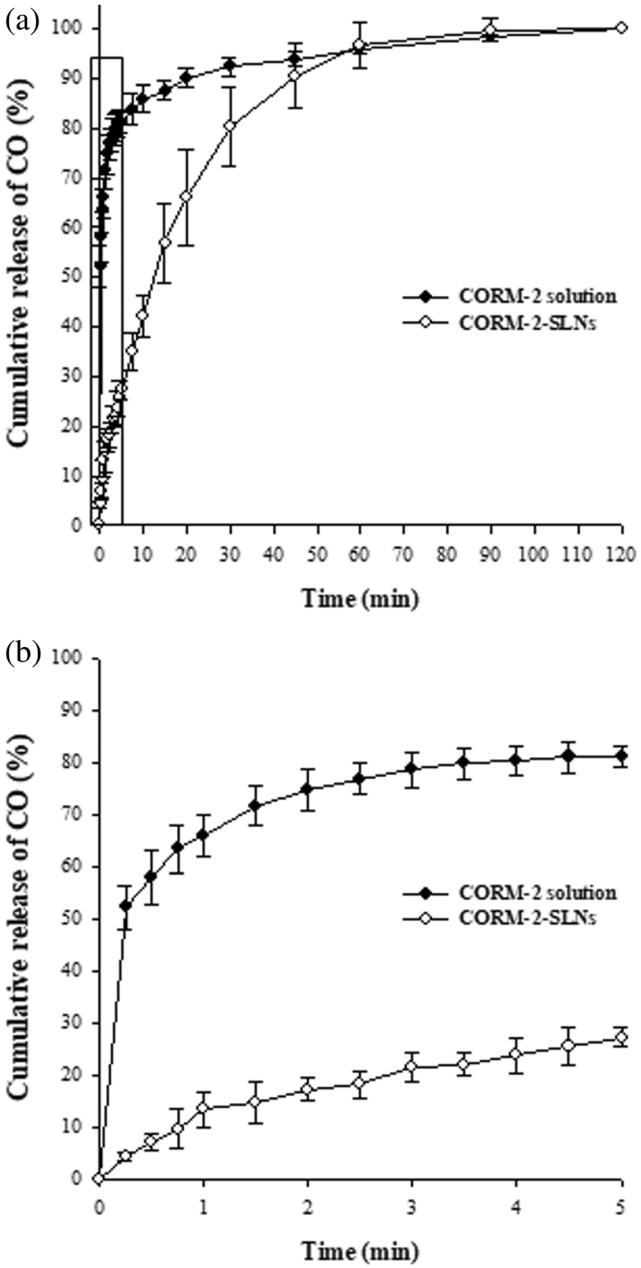

Fig. 2 Comparison of CO release between CORM-2-SLNs and CORM-2-S. **a** Release of CO from CORM-2-SLNs and CORM-2-S for 120 min. **B** Initial release of CO for 5 min. Data are expressed as mean ± SD ($N = 3$)

Table 2 Physicochemical properties of blank SLNs and CORM-2-SLNs

Formulation	Particle size (nm)	Polydispersity index	Zeta potential (Mv)	Incorporation efficiency (%)
Blank SLNs	119.4 ± 2.5	0.101 ± 0.023	− 19.9 ± 0.6	–
CORM-2-SLNs	119.5 ± 3.2	0.085 ± 0.006	− 3.7 ± 0.4	94.0 ± 0.7

Data are expressed as the mean ± SD ($N = 3$)

Blank SLNs solid lipid nanoparticles without incorporating CORM-2, *CORM-2-SLNs* CORM-2 containing solid lipid nanoparticles

Table 3 Storage stability of CORM-2 SLNs at 4 °C

Days	Particle Size (nm)	PDI	Zeta potential (mV)	CO release (%)
0	119.5 ± 3.2	0.085 ± 0.007	− 3.7 ± 0.4	100.0 ± 2.7
3	122.3 ± 2.6	0.092 ± 0.014	− 3.5 ± 0.6	98.3 ± 3.1
7	119.2 ± 4.3	0.103 ± 0.028	− 4.0 ± 1.2	99.2 ± 4.5
14	125.6 ± 3.7	0.087 ± 0.021	− 3.7 ± 0.6	97.6 ± 1.5
21	123.4 ± 4.0	0.112 ± 0.020	− 4.2 ± 1.7	96.8 ± 3.2
28	125.0 ± 3.1	0.105 ± 0.011	− 3.0 ± 0.9	95.8 ± 2.6

Data are expressed as the mean ± SD ($N = 3$)

Moreover, CO release from CORM-2-SLNs was maintained above 95% for 28-day storage. Even though CORM-2-SLNs were stable at storage condition, the freshly prepared CORM-2-SLNs were used for animal studies.

Effect of CORM-2-S and CORM-2-SLNs on Mechanical Allodynia

Sham-operated animals were not statistically different from naïve animals (data not shown). Mechanical allodynia was developed in the ipsilateral paw after CCI when compared to their respective contralateral paws (Fig. 3). Rats in the injury group presented with a strong hypersensitivity to innocuous mechanical stimuli at day 7, a response that persisted up to day 14, consistent with previous reports [31]. The basal PWT for animals were roughly 42 g, and CCI-induced drastic reduction in PWT; PWT were 16.9 ± 2.5, 14.6 ± 3.56, 14.17 ± 3.97, and 14.8 ± 3.8 at 1, 3, 7, and 14 days, respectively, in the injury group (CCI animals treated with at a dose of 10 mg/kg 5% dextrose, ip).

PWT in the PGB-treated group were 17.31 ± 0.32, 19.12 ± 1.57, 22.33 ± 2.63, and 29.11 ± 4.68 and in CORM-2-S-treated group were 18.4 ± 2.67, 22.01 ± 2.20, 24.8 ± 2.71, and 32.0 ± 1 at 1, 3, 7, and 14 days, respectively. This indicates that animals receiving repeated administration of 10 mg/kg PGB and 10 mg/kg CORM-2-S for 7 days exhibited decreased hypersensitivity to innocuous mechanical stimuli between days 3 and 14. However, significant difference was not observed between these two groups. PWT in the CORM-2-SLN-treated group were 21.4 ± 0.98, 26.33 ± 1.1, 32.1 ± 1.16, and 40 ± 1.58 at 1, 3, 7, and 14 days, respectively, suggesting that

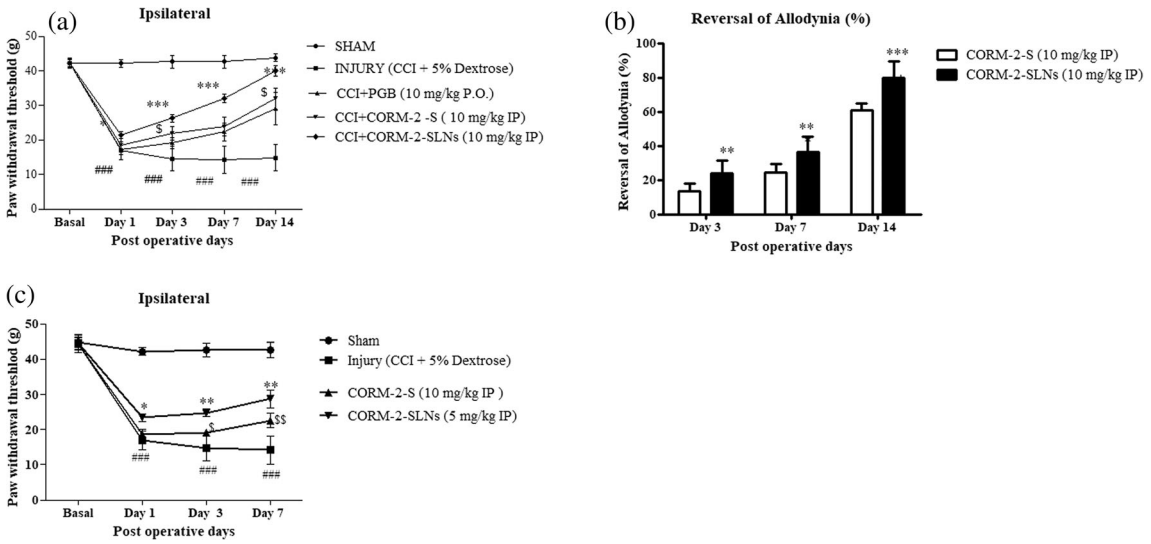

Fig. 3 Effects of PGB (10 mg/kg/day, po), CORM-2-S (10 mg/kg/day, ip), and CORM-2-SLNs (10 mg/kg/day, ip) on mechanical allodynia evoked by chronic constriction injury (CCI) in rats. Paw withdrawal threshold (PWT) was measured to check mechanical allodynia in hind limbs and ipsilateral paw. **a** PWT (g) in ipsilateral at dose 10 mg/kg, po, for PGB and 10 mg/kg, ip, for both CORM-2-S and CORM-2-SLNs. **b** Measurement of reversal of allodynia percentage by both CORM-2-S and CORM-2-SLNs. **c** Mechanical allodynia result obtained for CORM-2-S (10 mg/kg ip) and CORM-2-SLNs (5 mg/kg ip). PWT was measured 1 day before surgery and days 1, 3, 7, and 14 after surgery. However, during dose optimization, PWT was measured up to 1 week. Sham-operated rats were subjected to the same surgical procedure without ligation. Data represents the mean ± SD for six rats in each group. Data were analyzed by two-way ANOVA followed by Bonferroni post hoc test. (*$P < 0.05$, **$P < 0.01$, and ***$P < 0.001$ indicating statistically significant effect of CORM-2-SLNs over CORM-2-S, and *$P < 0.05$ and $^{\$\$}P < 0.001$ symbolizes the effects of CORM-2-S over injury group)

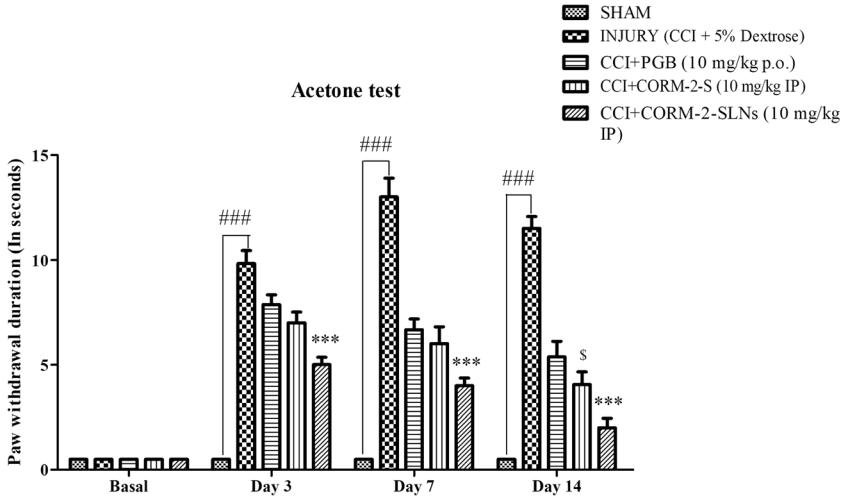

Fig. 4 Effects of PGB (10 mg/kg/day, po), CORM-2-S (10 mg/kg/day, ip), and CORM-2-SLNs (10 mg/kg/day, ip) on the attenuation of chronic constriction injury induced cold allodynia [increased paw withdrawal duration (PWDs) to a drop of acetone]. Data represents the mean ± SD for six rats in each group. Data were analyzed by two-way ANOVA followed by Bonferroni post hoc test. (*$P < 0.05$, **$P < 0.01$, and ***$P < 0.001$ indicating statistically significant effect of CORM-2-SLNs over CORM-2-S, and $^{###}P < 0.001$ symbolizes the significant increase in PWD in injury group compared to sham operated animals)

rats in the CORM-2-SLNs (10 mg/kg) treatment group exhibited significantly less hypersensitivity to mechanical allodynia compared with the PGB- and CORM-2-S-treated groups starting on day 3 [Fig. 3a (*$P < 0.05$ and ***$P < 0.001$)]. Additionally, the allodynia reversal rate was calculated in an ipsilateral paw from the PWT value obtained at different time points and was significantly higher in the CORM-2-SLNs (10 mg/kg)-treated group compared to the CORM-2-S (10 mg/kg)-treated group (Fig. 3b). At day 14, 80% and 60% of allodynia was eliminated by CORM-2-SLNs and CORM-2-S, respectively (Formula 2).

$$\text{Reversal of allodynia}\% = \frac{\text{Post-dose threshold} - \text{Pre-dose threshold}}{\text{Naive threshold} - \text{Pre-dose threshold}} \times 100 \quad (2)$$

These results suggest that animals treated with both CORM-2-S (10 mg/kg) and CORM-2-SLNs (10 mg/kg) were protected against mechanical allodynia induced by

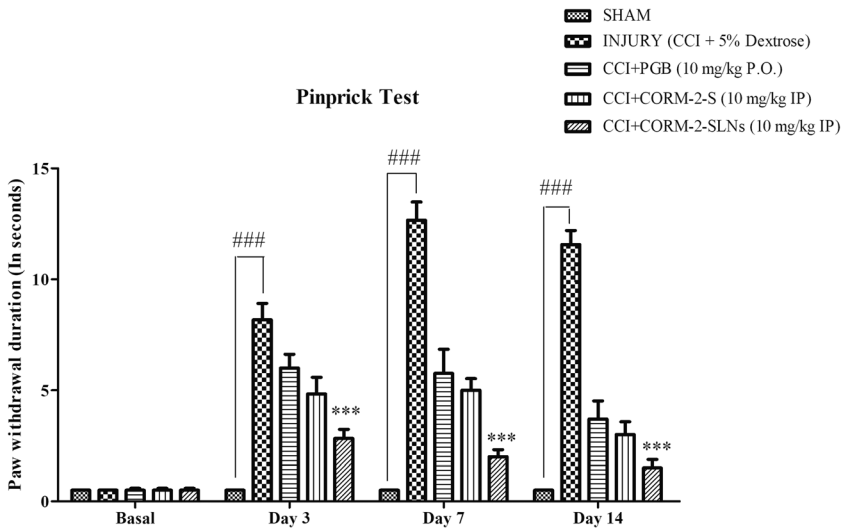

Fig. 5 Effects of PGB (10 mg/kg/day, po), CORM-2-S (10 mg/kg/day, ip), and CORM-2-SLNs (10 mg/kg/day, ip) on the attenuation of chronic constriction injury induced mechanical hyperalgesia (increased paw withdrawal duration to a pinprick). Data represents the mean ± SD for six rats in each group. Data were analyzed by two way ANOVA followed by Bonferroni post hoc test. (*$P < 0.05$, **$P < 0.01$, and ***$P < 0.001$ indicating statistically significant effect of CORM-2-SLNs over CORM-2-S, and $^{###}P < 0.001$ symbolizes the significant increase in PWD in injury group compared to sham operated animals)

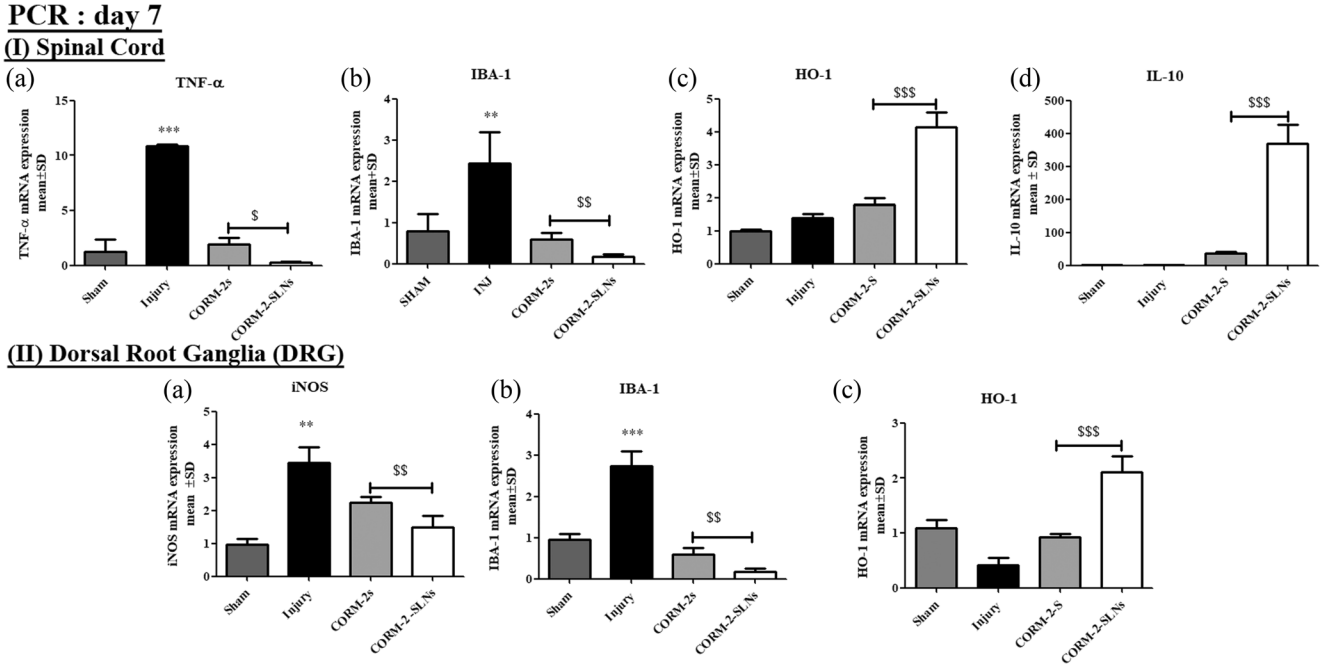

Fig. 6 Effects of CORM-2-S (10 mg/kg/day, ip) and CORM-2-SLNs (10 mg/kg/day, ip) on mRNA gene expression at 7 days after injury. **I** mRNA gene expression in spinal cord. **II** mRNA gene expression in dorsal root ganglion (DRG). In upper panel, A = TNF-α mRNA expression, B = IBA-1 mRNA expression, and C = HO-1 mRNA expression, and D = IL-10 mRNA expression, respectively, in lumbar spinal cord. While in lower panel, A = iNOS mRNA expression, B = IBA-1 mRNA expression, and C = HO-1 mRNA expression, respectively, in DRG. Data represents the mean ± SD for three rats per group. Data were analyzed by one way ANOVA followed by Tukey: compares all pairs of column ($^{\$}P < 0.05$ and $^{\$\$}P < 0.01$ denotes statistically significant effects of CORM-2-SLNs over CORM-2-S and $^{**}P < 0.01$ and $^{***}P < 0.001$ denotes significant expression of inflammatory markers in injury group)

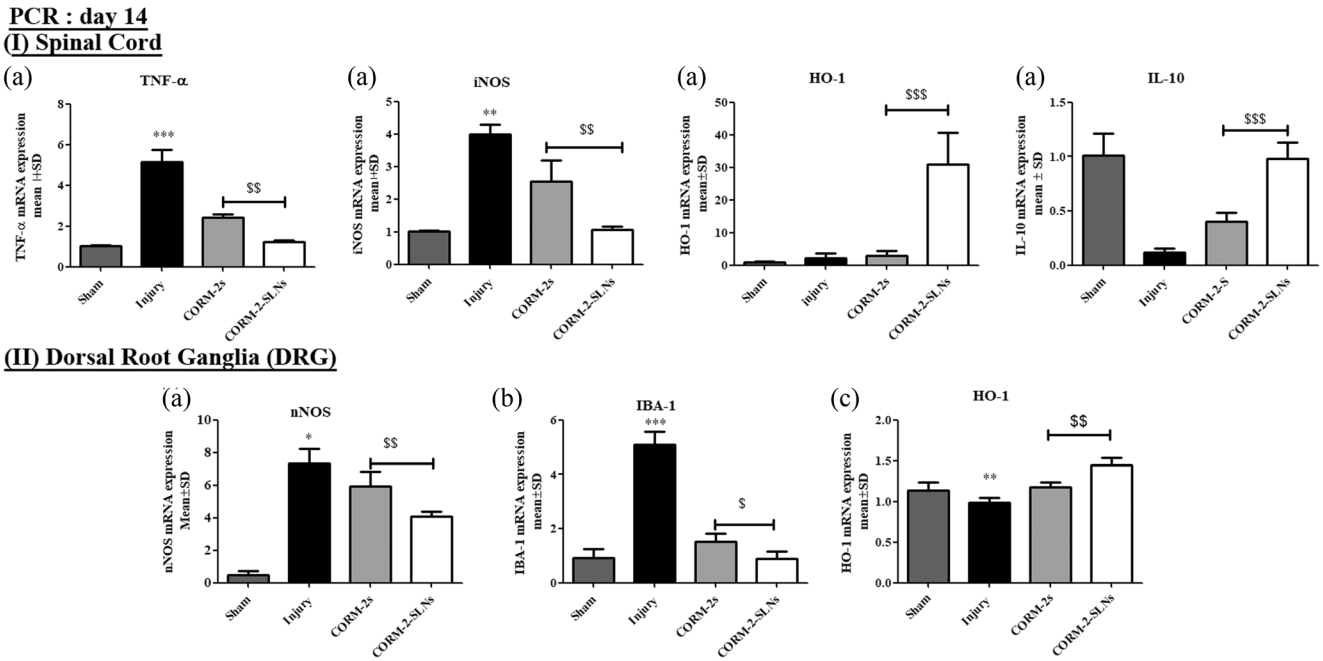

Fig. 7 Effects of CORM-2-S (10 mg/kg/day, ip) and CORM-2-SLNs (10 mg/kg/day, ip) on mRNA gene expression at 14 days after injury. **I** mRNA gene expression in spinal cord. **II** mRNA gene expression in dorsal root ganglion (DRG). In upper panel, A = TNF-α mRNA expression, B = iNOS mRNA expression, C = HO-1 mRNA expression, and D = IL-10 mRNA expression, respectively, in lumbar spinal cord. While in lower panel, A = nNOS mRNA expression, B = IBA-1 mRNA expression, and C = HO-1 mRNA expression, respectively, in DRG. Data represents the mean ± SD for three rats per group. Data were analyzed by one-way ANOVA followed by Tukey: compares all pairs of column. ($^{\$}P < 0.05$ and $^{\$\$}P < 0.01$ denotes statistically significant effects of CORM-2-SLNs over CORM-2-S and $^{**}P < 0.01$ and $^{***}P < 0.001$ denotes significant expression of inflammatory markers in injury group)

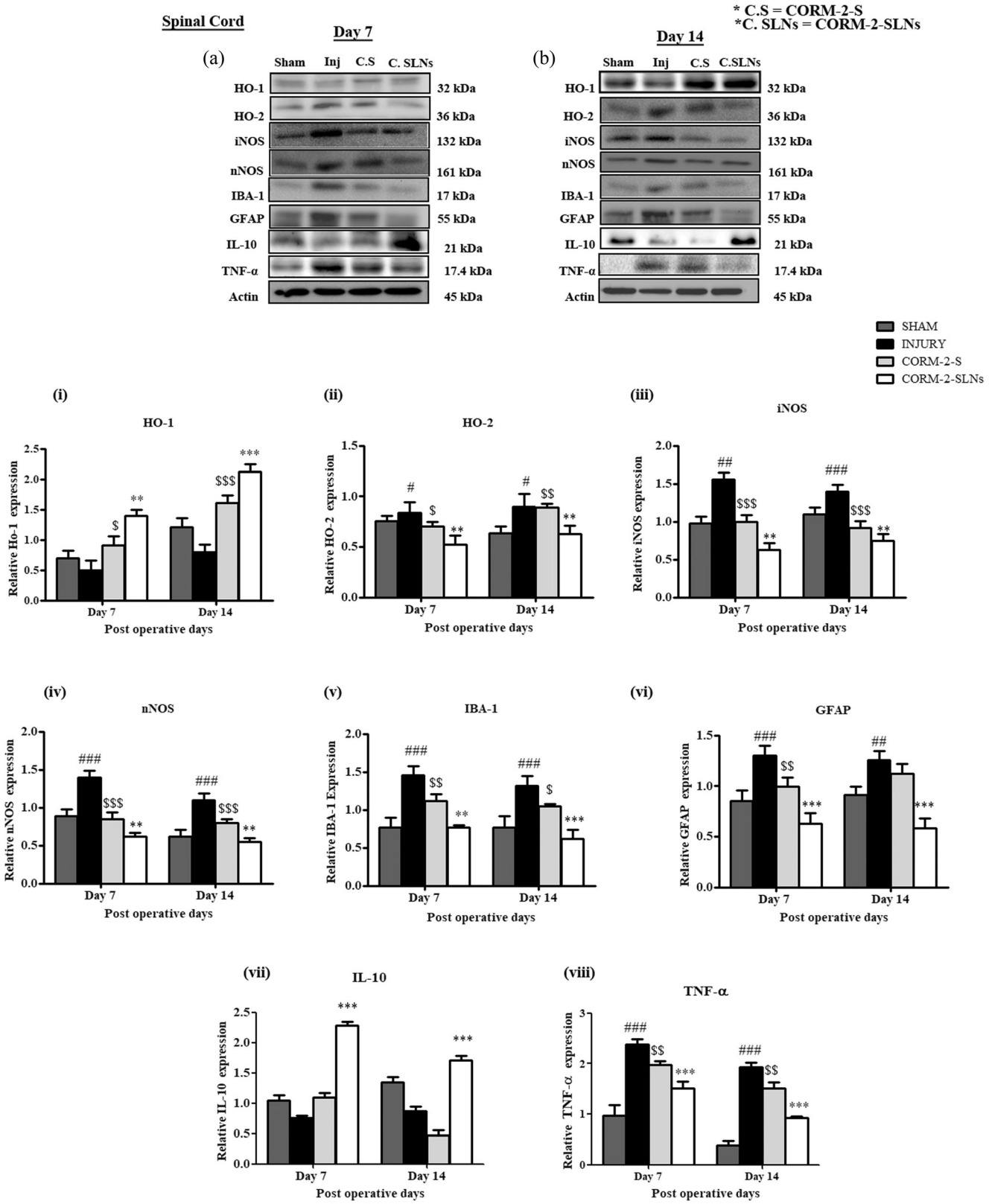

CCI of the sciatic nerve. However, CORM-2-SLNs conferred a greater ability to prevent mechanical allodynia than CORM-2-S.

To determine the superiority of treatment with CORM-2-SLNs, we also compared the effects of low-dose CORM-2-SLNs (5 mg/kg, ip) with CORM-2-S

◀ **Fig. 8** Effects of CORM-2-S (10 mg/kg/day, ip) and CORM-2-SLNs (10 mg/kg/day, ip) on the expression of HO-1, HO-2, iNOS, nNOS IBA-1, GFAP, IL-10, and TNF-α proteins in the spinal cord, at days 7 and 14 after injury. **a**, **b** Band intensity of different proteins at days 7 and 14, respectively, in spinal cord and below down showing relative protein level. i = HO-1 expression level, ii = HO-2 expression level, iii = iNOS expression level, iv = nNOS expression level, v = IBA-1 expression level, vi = GFAP expression level, vii = IL-10 expression level, and viii = TNF-α expression level. Protein bands were taken at the same exposure time. Band intensities were quantified by ImageJ software and normalized with β-actin. Data represents mean ± SD for three rats per group. Data were analyzed by two-way ANOVA followed by Bonferroni post hoc test. (*$P < 0.05$, **$P < 0.01$ and ***$P < 0.001$ denotes statistically significant effects of CORM-2-SLNs over CORM-2-S, $^{\$}P < 0.05$, $^{\$\$}P < 0.01$, and $^{\$\$\$}P < 0.001$ denotes effects of CORM-2-S over injury group and $^{\#}P < 0.05$, $^{\#\#}P < 0.01$, and $^{\#\#\#}P < 0.001$ denotes significant expression of inflammatory protein in injury group over sham group)

(10 mg/kg, ip) using the same animal model. Treatment with CORM-2-SLNs (5 mg/kg) increased PWT to 20.34 ± 1.10, 24.75 ± 1.04, and 28.70 ± 2.60 at 1, 3, and 7 days, respectively. However, PWT values were 18.65 ± 1.32, 19.12 ± 0.63, and 22.6 ± 2.02 at 1, 3, and 7 days in the CORM-2-S (10 mg/kg ip)-treated group. These results suggest that animals receiving low-dose CORM-2-SLNs presented with less hypersensivity to innocuous mechanical stimuli from day 3 to the last day of the experiment (day 7), in comparison to CORM-2-S-treated group (Fig. 3c). In addition, rats treated with CORM-2-SLNs (10 mg) exhibited less hypersensitivity to mechanical allodynia compared with rats treated with CORM-2-SLNs (5 mg) from days 3 to 7 of the experiment (Fig. 3a, c).

Effect of CORM-2-S and CORM-2-SLNs on Cold Allodynia

A markedly increased withdrawal reflex was observed in injury-only group as compared to sham-operated one, upon application of an acetone drop on the mid-plantar surface of the left hind limb. Paw withdrawal durations (PWD) were 9.83 ± 0.60 s, 13.00 ± 0.89 s, and 11.50 ± 0.56 s at 3, 7, and 14 days, respectively, in nerve-ligated group while baseline was 0.5 s. It was significantly subsided by PGB to 7.86 ± 0.47, 6.66 ± 0.51, and 5.36 ± 0.75 and by CORM-2-S to 7.0 ± 0.51, 6.0 ± 0.81, and 4.0 ± 0.61 at 3, 7, and 14 days, respectively. However, significant difference was not observed between PGB and CORM-2-S. In contrast, paw withdrawal durations in CORM-2-SLNs treated group were 5.0 ± 0.35, 4.0 ± 0.36, and 2.0 ± 0.45 at days 3, 7, and 14 days, respectively (Fig. 4), suggesting that CORM-2SLNs has significantly prominent anti-allodynic effects compared to PGB and CORM-2-S.

Effect of CORM-2-S and CORM-2-SLNs on Mechanical Hyperalgesia

The hyperalgesia induced by manual pricking at the mid plantar surface of the hind limb was prominent from days 3 to 14 in injury group. In which, PWD markedly increased from presurgery baseline of 0.5 s to 8.16 ± 0.74, 12.66 ± 0.81, and 11.56 ± 0.63 at 3, 7, and 14 days, respectively. It was significantly subsided by PGB to 6.00 ± 0.63, 5.75 ± 1.09, and 3.7 ± 0.8 and by CORM-2-S to 4.83 ± 0.75, 5.00 ± 0.53, and 3.0 ± 0.58 at 3, 7, and 14 days, respectively. However, significant difference was not observed between PGB and CORM-2-S. In contrast, CORM-2-SLNs dramatically decreased PWD to 2.83 ± 0.40 s, 2.0 ± 0.32 s, and 1.5 ± 0.38 s at 3, 7, and 14 days, respectively (Fig. 5). Thus, even though both PGB and CORM-2-S significantly lessened the PWD in both acetone test and pinprick test, it was less prominent then CORM-2-SLNs one. So, CORM-2-SLNs conferred greatest ability to attenuate mechanical allodynia and mechanical hyperalgesia. Based on the above nociceptive test result, significant difference was not observed between PGB and CORM-2-S treatment, so we did not include PGB group in later biochemical assays.

Effects of CORM-2-S and CORM-2-SLNs on the Biochemical Markers of Neuropathic Pain in DRG and Spinal Cord

The results of behavioral experiments revealed that 10 mg/kg was the most effective test dose of CORM-2-SLNs and CORM-2-S; thus, rats receiving this dose were chosen for RT-PCR and western blot analyses. Since behavioral tests revealed that pain was most severe at day 7, biochemical markers of neuropathic pain were measured in both the DRGs and dorsal horns of L4–L6 spinal cords at days 7 and 14 after injury.

TNF-α, iNOS, nNOS, IBA-1, HO-1, and IL-10 mRNA Expression

RT-PCR analysis revealed significant increases in the TNF-α levels in the injured spinal cord, on days 7 ($P < 0.001$; Fig. 6I-A) and 14 ($P < 0.001$; Fig. 7I-A). Post-CCI downregulation of TNF-α levels in CCI plus CORM-2-SLNs (10 mg/kg) were significant on both experimental days 7 ($^{\$}P < 0.05$; Fig. 6I-A) and 14 ($^{\$\$}P < 0.01$; Fig. 7I-A).

On day 7, the levels of iNOS and nNOS increased in CCI rats, which remained high on day 14 post-CCI ($^{\$}P < 0.05$, $^{\$\$}P < 0.01$; Figs. 6II-A, 7I-B, II-A). Treatment with CORM-2-SLNs 10 mg/kg was the most effective in reducing iNOS and nNOS levels on both experimental days. Increased IBA-1 levels were observed in both the DRG and spinal cord of CCI rats on days 7 and 14 ($^{\$}P < 0.05$, $^{\$\$}P < 0.01$; Figs. 6I-B, II-B

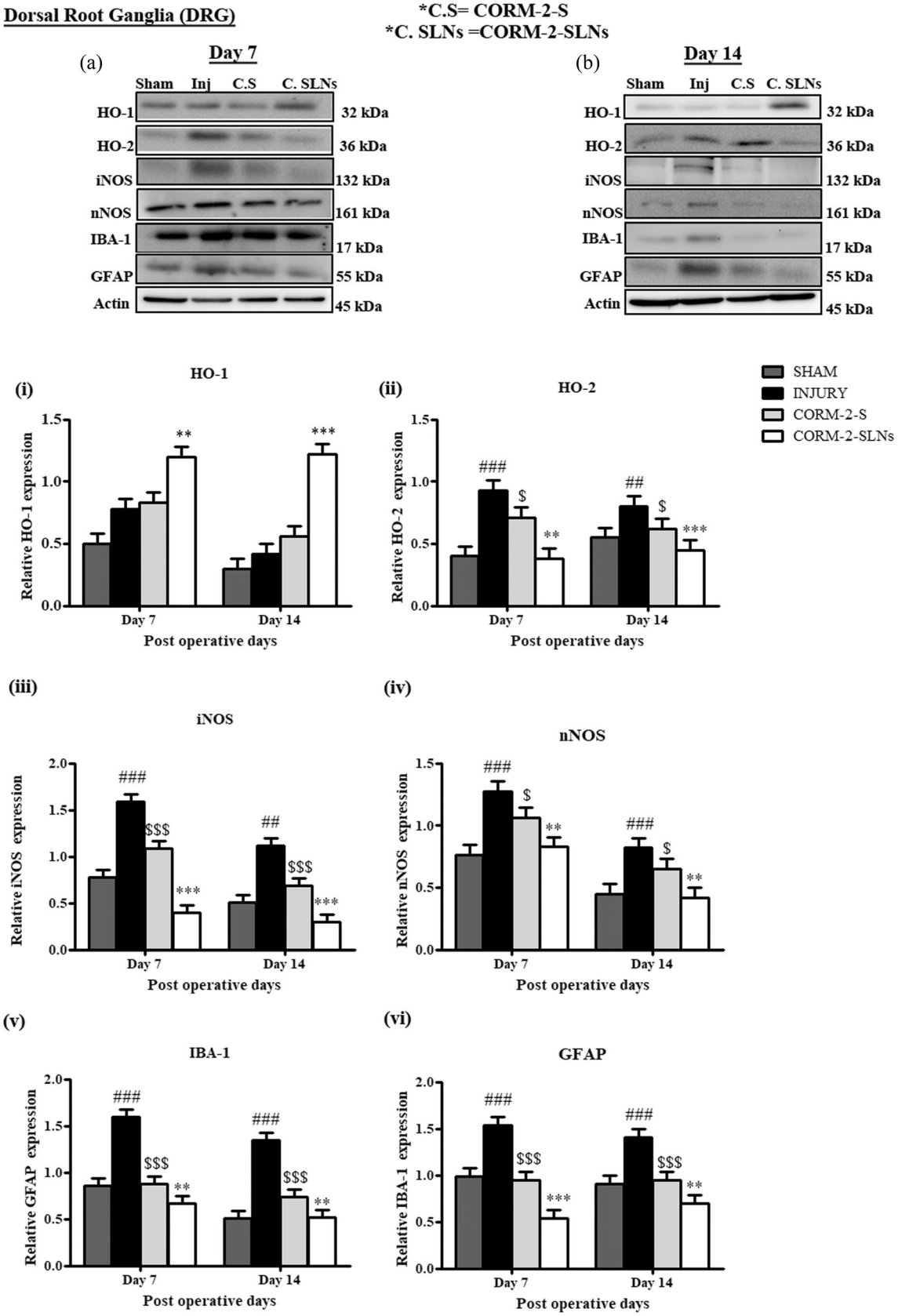
Dorsal Root Ganglia (DRG)
*C.S= CORM-2-S
*C. SLNs =CORM-2-SLNs
(a)
Day 7
Sham Inj C.S C. SLNs
HO-1 32 kDa
HO-2 36 kDa
iNOS 132 kDa
nNOS 161 kDa
IBA-1 17 kDa
GFAP 55 kDa
Actin 45 kDa
(b)
Day 14
Sham Inj C.S C. SLNs
HO-1 32 kDa
HO-2 36 kDa
iNOS 132 kDa
nNOS 161 kDa
IBA-1 17 kDa
GFAP 55 kDa
Actin 45 kDa
SHAM
INJURY
CORM-2-S
CORM-2-SLNs
(i) HO-1
Relative HO-1 expression
Day 7
Day 14
Post operative days
(ii) HO-2
Relative HO-2 expression
Day 7
Day 14
Post operative days
(iii) iNOS
Relative iNOS expression
Day 7
Day 14
Post operative days
(iv) nNOS
Relative nNOS expression
Day 7
Day 14
Post operative days
(v) IBA-1
Relative GFAP expression
Day 7
Day 14
Post operative days
(vi) GFAP
Relative IBA-1 expression
Day 7
Day 14
Post operative days

◀ **Fig. 9** Effects of CORM-2-S (10 mg/kg/day, ip) and CORM-2-SLNs (10 mg/kg/day, ip) on the expression of HO-1, HO-2, INOS, nNOS, IBA-1, and GFAP proteins in dorsal root ganglia (DRG), at days 7 and 14 after injury. **a**, **b** Band intensity of different proteins at days 7 and 14, respectively, in dorsal root ganglia and below down showing relative protein level. i = HO-1 expression level, ii = HO-2 expression level, iii = iNOS expression level, iv = nNOS expression level, v = IBA-1 expression level, and vi = GFAP expression level. Protein bands were taken at the same exposure time. Band intensities were quantified by ImageJ software and normalized with B-actin. Data represents mean ± SD for three rats per group. Data were analyzed by two-way ANOVA followed by Bonferroni post hoc test. (*$P < 0.05$, **$P < 0.01$, and ***$P < 0.001$ denotes statistically significant effects of CORM-2-SLNs over CORM-2-S, $^{\$}P < 0.05$, $^{\$\$}P < 0.01$, and $^{\$\$\$}P < 0.001$ denotes effects of CORM-2-S over injury group and $^{\#}P < 0.05$, $^{\#\#}P < 0.01$ and $^{\#\#\#}P < 0.001$ denotes significant expression of inflammatory protein in injury group)

and 7II-B). Seven days of treatment with CORM-2-SLNs (10 mg/kg) resulted in the most significant reduction of the IBA-1 level on days 7 and 14 ($^{\$}P < 0.05$, $^{\$\$}P < 0.01$; Figs. 6I-B, II-B and 7II-B). In contrast, the levels of HO-1 and IL-10 were significantly decreased on days 7 and 14 post-CCI compared with the sham group (Figs. 6I-C, D, II-C; 7I-C, D, II-C). Groups treated with either CORM-2-S or CORM-2-SLNs revealed significant elevation of HO-1 and IL-10, however, treatment with CORM-2-SLNs resulted in greater differences ($^{\$}P < 0.05$, $^{\$\$}P < 0.01$, and $^{\$\$\$}P < 0.001$; Figs. 6I-C, D, II-C, 7I-C, D, II-C).

iNOS, nNOS, IBA-1, HO-1, HO-2, GFAP, IL-10, and TNF-α Protein Expression

Western blot analyses revealed significant changes in the levels of HO-1, HO-2, iNOS, nNOS, IBA-1, GFAP, and TNF-α in the spinal cord (Fig. 8) and DRGs (Fig. 9), on days 7 and 14 post-CCI compared with the sham group. The levels of HO-2, iNOS, nNOS, IBA-1, GFAP, and TNF-α proteins significantly increased in the spinal cord and DRGs of CCI rats on days 7 and 14, while HO-1 and IL-10 decreased in CCI rats on days 7 and 14. In both the spinal cord and DRG, we determined that IBA-1 expression was higher at day 7 than 14, while the expression of GFAP was slightly greater at day 14 than at 7 [32]. Repeated intraperitoneal injection of CORM-2-S (10 mg/kg) and CORM-2-SLNs (10 mg/kg) led to reductions in HO-2, iNOS, nNOS, IBA-1, GFAP, and TNF-α levels and increases in the levels of HO-1 and IL-10 on days 7 and 14 (*$P < 0.05$, **$P < 0.01$, and ***$P < 0.001$; Figs. 8 and 9). However, animals receiving CORM-2-SLNs, 10 mg/kg ip, revealed more significant reductions of HO-2, iNOS, nNOS, IBA-1, GFAP, and TNF-α protein levels and a more significant elevation of HO-1 and IL-10, compared with the CORM-2-S-treated group. These results indicate that CORM-2-SLNs have a greater ability to prevent mechanical allodynia induced by CCI than CORM-2-S.

Discussion

It has been reported that nanocarriers are useful in the drug-delivery process. In this study, we prepared solid lipid nanoparticles as CORM-2 carriers to overcome its dissolution challenges. CORM-2 was incorporated into the lipid core of CORM-2-SLNs to achieve the slow release of CO with improved solubility (Fig. 10a, b). Here, CORM-2 and CORM-2-SLNs are CO carriers that release CO into target tissues. Previous studies have reported that intraperitoneal administration of 10 mg/kg of inactivated CORM-2 (iCORM-2) or iCORM-3 had no significant effect on the attenuation of principal symptoms of neuropathic pain (mechanical allodynia and mechanical hyperalgesia) [28], and inactive molecules (iCORM-2 or iCORM-3) showed no pharmacological effects in diverse animal models emphasizing that transition metal carbonyls were responsible for the effects. Thus, we did not

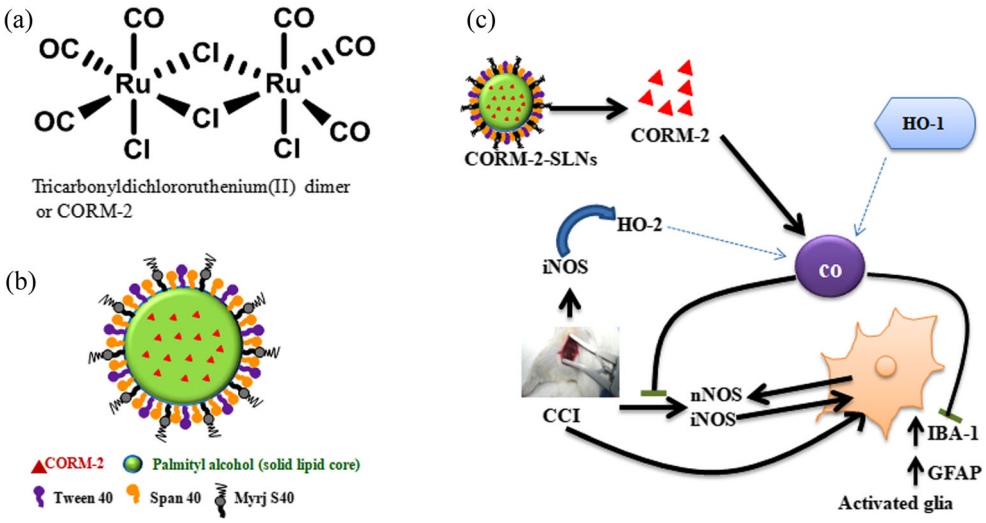

Fig. 10 Graphical summary, demonstrating the attenuation of neuropathic pain by CORM-2-SLNs. **a** Molecular structure of CORM-2 molecule. **b** CORM-2 loaded solid lipid nanoparticle. **c** Mechanism of CO release from CORM-2-SLNs and its pain-relieving mechanism

include the inactive form of CORM as a control in these experiments. The assessment of blood COHb levels in disease models has not been proven reliable due to the low solubility of CO in water and its poor sensitivity at lower CO concentration [7]. It has also been reported that no elevation of basal COHb levels at therapeutic doses after intraperitoneal or intravenous injection of CORM-2 was detected [7, 25]. Additionally it has been considered to be difficult to prove CO release by measuring the amount of CO in tissue samples. For these reasons, we did not measure in vivo COHb levels after administration of CORM-2-S and CORM-2-SLNs, and instead focused mainly on in vitro CO release from CORM-2-S and CORM-2-SLNs, and in vivo pharmacological effects in a rat CCI model.

Our findings reveal that CORM-2-SLNs were superior to CORM-2-S in alleviating mechanical allodynia and mechanical hyperalgesia by upregulating IL-10 and HO-1 and downregulating iNOS/nNOS, HO-2, IBA-1, GFAP, and TNF-α expression (Fig. 10c). An in vitro CO release profile test revealed that CO release from CORM-2-SLNs occurred more slowly than from CORM-2-S. Based on our dose-optimization study and literature reviews [27], we chose 10 mg/kg/day dose to compare the efficacy of CORM-2-SLNs and CORM-2-S treatment. In order to confirm the superior effect of CORM-2-SLNs; however, we also compared 5-mg dose of CORM-2-SLNs with 10-mg dose of CORM-2-S (Fig. 3c).

In the present study, both CORM-2-S and CORM-SLNs led to reductions in mechanical allodynia and mechanical hyperalgesia by reducing expression of iNOS/nNOS and inflammatory mediators (TNF-α, IBA-1, GFAP) and enhancing expression of HO-1 and IL-10. The anti-allodynic and anti-hyperalgesic effects of CORM-2-S and CORM-SLNs may result from the therapeutic benefits of CO. Although the possible mechanisms implicated in the anti-allodynic and anti-hyperalgesic effects demonstrated by CO remains unknown, we suggest several possibilities based on our results: (i) inhibition of glial cell activation, (ii) suppression of microglia activation and release of proinflammatory cytokines, (iii) inhibition of iNOS/nNOS activation, and (iv) activation of the HO-1/CO signaling pathway.

Glial cells (e.g., astrocytes and microglia) in the spinal cord may play an important role in the induction and maintenance of neuropathic pain [33, 34]. Additionally, activated astrocytes may express the cytokine GFAP after injury and GFAP upregulation after injury has been report to be involved in the maintenance of neuropathic pain [35]. Our data are in agreement with previous studies and revealed the intense levels of GFAP in CCI group on both days 7 and 14. In contrast, both CORM-2-S (10 mg/kg) and CORM-s-SLNs (10 mg/kg) diminished the GFAP levels in CCI rats, with greater effects observed in the CORM-2-SLN-treated group. Furthermore, activation of microglia in DRGs and the spinal cord plays a critical role in neuropathic pain. After nerve injury, microglia release large amounts of proinflammatory cytokines including TNF-α, IBA-1, and iNOS which are involved in the development of neuropathic pain by sensitizing nerve fibers [36–40]. In this study, we found that TNF-α, IBA-1, and iNOS were elevated in the spinal cord and DRGs of CCI animals on days 7 and 14. Treatment with CORM-2-SLNs (5 mg/kg and 10 mg/kg) decreased TNF-α, IBA-1, and iNOS levels more significantly compared with CORM-2-S (10 mg/kg) treatment of CCI animals.

Nitric oxide (NO) regulates the maintenance of neuropathic pain by activating the spinal NO-soluble guanylyl cyclase (sGC)/cyclic guanosine 3′,5′-monophosphate (cGMP)-dependent protein kinase (PKG) signaling pathway. This pathway can be triggered primarily by iNOS and nNOS. sGC and PKG enzymes are involved in the transduction of NO in the spinal cord and DRGs at the time of nerve injury. A study reported that inhibition of iNOS/nNOS and NO-sGC-PKG pathways results in the attenuation of neuropathic pain in peripheral nerve injury [41]. Moreover, endogenously synthesized CO is capable of diminishing the synthesis of nNOS and iNOS and attenuating neuropathic pain by blocking the microglial activation pathway. In accordance with this evidence, our results also demonstrated that both CORM-2-S and CORM-SLNs could lead to reduced iNOS and nNOS levels in the spinal cord and DRGs, but CORM-2-SLNs was superior to CORM-2-S in mitigating the level of iNOS and nNOS in CCI animals.

Activation of the HO-1/CO signaling pathway has been reported to play an important role in attenuating neuropathic pain [2]. Excessive NO generation could also be inhibited by the HO-1/CO pathway by constant inhibition of iNOS/nNOS expression [33].

HO-1 is known to participate in the attenuation of acute inflammatory pain [42], while HO-2 exerts a pro-nocicetive effect during neuropathic pain [43]. It has been reported that iNOS is needed to upregulate HO-2 after injury [44]. In this study, HO-1 expression decreased after CCI surgery in the DRGs and spinal cord and IL-10 expression decreased in the spinal cord, while HO-2 expression increased on days 7 and 14. Both CORM-2-S and CORM-2-SLNs also led to decreases in HO-2 levels and increases in HO-1 and IL-10 levels on days 7 and 14; however, CORM-2-SLNs resulted in greater effects.

Conclusion

Our results suggest that (i) CO incorporated in solid lipid nanoparticles can be released slowly and (ii) CORM-2-SLNs could provide more rapid and effective reduction of mechanical allodynia and mechanical hyperalgesia compared with CORM-2-S. These effects were mediated by (i) increase in

the mRNA and protein levels of HO-1 and IL-10 and (ii) decrease in the expression of iNOS/nNOS and markers of glial cells and microglia (TNF-α, IBA-1, GFAP) related to neuroinflammation.

Acknowledgements This research was supported by the National Research Foundation (NRF) of Korea (NRF2017R1C1B1011397) and Korea Health Technology Research and Development Project, Ministry for Health and Welfare Affairs (HI16C1559, HI18C0183). This work was supported by the Basic Science Research Program of the National Research Foundation of Korea (NRF) funded by the Ministry of Science and ICT (NRF-2017R1A2B4006458).

Author Contributions IBH and JKK conceived and directed the project. IBH, HPJ, and HK designed the whole experimental plan. HPJ, MJJ, HC, JK, SK, and KW carried out the experiments. SBK, SS, and KTK analyzed the data and interpreted the result. IBH, HPJ, SBK, and SK wrote the paper. All authors reviewed the manuscript.

Compliance with Ethical Standards

Competing Interests The authors declare that they have no competing interests.

Publisher's Note Springer Nature remains neutral with regard to jurisdictional claims in published maps and institutional affiliations.

References

1. Jurga AM, Piotrowska A, Makuch W, Przewlocka B, Mika J (2017) Blockade of P2X4 receptors inhibits neuropathic pain-related behavior by preventing MMP-9 activation and, consequently, pronociceptive interleukin release in a rat model. Front Pharmacol 8:48
2. Riego G, Redondo A, Leánez S, Pol O (2018) Mechanism implicated in the anti-allodynic and anti-hyperalgesic effects induced by the activation of heme oxygenase 1/carbon monoxide signaling pathway in the central nervous system of mice with neuropathic pain. Biochem Pharmacol 148:52–63
3. Jensen TS, Baron R, Haanpää M, Kalso E, Loeser JD, Rice AS, Treede R-D (2011) A new definition of neuropathic pain. Pain 152(10):2204–2205
4. Finnerup NB, Haroutounian S, Kamerman P, Baron R, Bennett DL, Bouhassira D, Cruccu G, Freeman R et al (2016) Neuropathic pain: an updated grading system for research and clinical practice. Pain 157(8):1599–1606
5. Ryter SW, Otterbein LE (2004) Carbon monoxide in biology and medicine. Bioessays 26(3):270–280
6. Wu L, Wang R (2005) Carbon monoxide: endogenous production, physiological functions, and pharmacological application. Pharmacol Rev 57(4):585–630
7. Motterlini R, Otterbein LE (2010) The therapeutic potential of carbon monoxide. Nat Rev Drug Discov 9(9):728–743
8. Otterbein LE, Bach FH, Alam J, Soares M, Lu HT, Wysk M, Davis RJ, Flavell RA et al (2000) Carbon monoxide has anti-inflammatory effects involving the mitogen-activated protein kinase pathway. Nat Med 6(4):422–428
9. Otterbein LE, Zuckerbraun BS, Haga M, Liu F, Song R, Usheva A, Stachulak C, Bodyak N et al (2003) Carbon monoxide suppresses arteriosclerotic lesions associated with chronic graft rejection and with balloon injury. Nat Med 9(2):183–190
10. Foresti R, Bani-Hani MG, Motterlini R (2008) Use of carbon monoxide as a therapeutic agent: promises and challenges. Intensive Care Med 34(4):649–658
11. Romao CC, Blättler WA, Seixas JD, Bernardes GJ (2012) Developing drug molecules for therapy with carbon monoxide. Chem Soc Rev 41(9):3571–3583
12. Marques AR, Kromer L, Gallo DJ, Penacho N, Rodrigues SS, Seixas JD, Bernardes GJ, Reis PM et al (2012) Generation of carbon monoxide releasing molecules (CO-RMs) as drug candidates for the treatment of acute liver injury: targeting of CO-RMs to the liver. Organometallics 31(16):5810–5822
13. Motterlini R (2007) Carbon monoxide-releasing molecules (CO-RMs): vasodilatory, anti-ischaemic and anti-inflammatory activities. Portland Press Limited
14. Motterlini R, Haas B, Foresti R (2012) Emerging concepts on the anti-inflammatory actions of carbon monoxide-releasing molecules (CO-RMs). Med Gas Res 2(1):28
15. Bunjes H (2010) Lipid nanoparticles for the delivery of poorly water-soluble drugs. J Pharm Pharmacol 62(11):1637–1645
16. Mehnert W, Mäder K (2001) Solid lipid nanoparticles: production, characterization and applications. Adv Drug Deliv Rev 47(2):165–196
17. Chenglin Y, Yiqun Y, Ye Z, Na L, Xiaoya L, Jing L, Ming J (2012) Self-assembly and emulsification of poly {[styrene-alt-maleic acid]-co-[styrene-alt-(N-3, 4-dihydroxyphenylethyl-maleamic acid)]}. Langmuir 28(25):9211–9222
18. Severino P, Andreani T, Macedo AS, Fangueiro JF, Santana MHA, Silva AM, Souto EB (2012) Current state-of-art and new trends on lipid nanoparticles (SLN and NLC) for oral drug delivery. J Drug Deliver 1:10
19. Müller RH, MaÈder K, Gohla S (2000) Solid lipid nanoparticles (SLN) for controlled drug delivery—a review of the state of the art. Eur J Pharm Biopharm 50(1):161–177
20. Natarajan JV, Nugraha C, Ng XW, Venkatraman S (2014) Sustained-release from nanocarriers: a review. J Control Release 193:122–138
21. Rippe B (1993) A three-pore model of peritoneal transport. Perit Dial Int 13(Suppl 2):S35–S38
22. Qureshi OS, Zeb A, Akram M, Kim M-S, Kang J-H, Kim H-S, Majid A, Han I et al (2016) Enhanced acute anti-inflammatory effects of CORM-2-loaded nanoparticles via sustained carbon monoxide delivery. Eur J Pharm Biopharm 108:187–195
23. Qureshi OS, Kim H-S, Zeb A, Choi J-S, Kim H-S, Kwon J-E, Kim M-S, Kang J-H et al (2017) Sustained release docetaxel-incorporated lipid nanoparticles with improved pharmacokinetics for oral and parenteral administration. J Microencapsul 34(3):250–261
24. Atkin AJ, Lynam JM, Moulton BE, Sawle P, Motterlini R, Boyle NM, Pryce MT, Fairlamb IJ (2011) Modification of the deoxymyoglobin/carbonmonoxy-myoglobin UV-Vis assay for reliable determination of CO-release rates from organometallic carbonyl complexes. Dalton Trans 40(21):5755–5761
25. Motterlini R, Clark JE, Foresti R, Sarathchandra P, Mann BE, Green CJ (2002) Carbon monoxide-releasing molecules: characterization of biochemical and vascular activities. Circ Res 90(2):e17–e24
26. Bennett GJ, Xie Y-K (1988) A peripheral mononeuropathy in rat that produces disorders of pain sensation like those seen in man. Pain 33(1):87–107
27. Thiagarajan VR, Shanmugam P, Krishnan UM, Muthuraman A (2014) Ameliorative potential of Vernonia cinerea on chronic constriction injury of sciatic nerve induced neuropathic pain in rats. An Acad Bras Cienc 86(3):1435–1450
28. Hervera A, Leánez S, Motterlini R, Pol O (2013) Treatment with carbon monoxide-releasing molecules and an HO-1 inducer enhances the effects and expression of μ-opioid receptors during

neuropathic pain. Anesthesiol: J Am Soc Anesthesiol 118(5):1180–1197
29. Shahid M, Subhan F, Ahmad N, Ullah I (2017) A bacosides containing Bacopa monnieri extract alleviates allodynia and hyperalgesia in the chronic constriction injury model of neuropathic pain in rats. BMC Complement Altern Med 17(1):293
30. Erichsen HK, Blackburn-Munro G (2002) Pharmacological characterisation of the spared nerve injury model of neuropathic pain. Pain 98(1–2):151–161
31. Zhou C, Shi X, Huang H, Zhu Y, Wu Y (2014) Montelukast attenuates neuropathic pain through inhibiting p38 mitogen-activated protein kinase and nuclear factor-kappa B in a rat model of chronic constriction injury. Anesth Analg 118(5):1090–1096
32. Guo C-H, Bai L, Wu H-H, Yang J, Cai G-H, Zeng S-X, Wang X, Wu S-X et al (2017) Midazolam and ropivacaine act synergistically to inhibit bone cancer pain with different mechanisms in rats. Oncol Rep 37(1):249–258
33. Berger JV, Deumens R, Goursaud S, Schäfer S, Lavand'homme P, Joosten EA, Hermans E (2011) Enhanced neuroinflammation and pain hypersensitivity after peripheral nerve injury in rats expressing mutated superoxide dismutase 1. J Neuroinflammation 8(1):33
34. Levy D, Höke A, Zochodne DW (1999) Local expression of inducible nitric oxide synthase in an animal model of neuropathic pain. Neurosci Lett 260(3):207–209
35. Kim D-S, Figueroa KW, Li K-W, Boroujerdi A, Yolo T, Luo ZD (2009) Profiling of dynamically changed gene expression in dorsal root ganglia post peripheral nerve injury and a critical role of injury-induced glial fibrillary acetic protein in maintenance of pain behaviors. Pain 143(1–2):114–122
36. Olmos G, Lladó J (2014) Tumor necrosis factor alpha: a link between neuroinflammation and excitotoxicity. Mediat Inflamm
37. Bijjem KRV, Padi SS, lal Sharma P (2013) Pharmacological activation of heme oxygenase (HO)-1/carbon monoxide pathway prevents the development of peripheral neuropathic pain in Wistar rats. Naunyn Schmiedeberg's Arch Pharmacol 386(1):79–90
38. Meller S, Dykstra C, Grzybycki D, Murphy S, Gebhart G (1994) The possible role of glia in nociceptive processing and hyperalgesia in the spinal cord of the rat. Neuropharmacology 33(11):1471–1478
39. Watkins LR, Milligan ED, Maier SF (2001) Glial activation: a driving force for pathological pain. Trends Neurosci 24(8):450–455
40. Raghavendra V, Tanga FY, DeLeo JA (2004) Complete Freunds adjuvant-induced peripheral inflammation evokes glial activation and proinflammatory cytokine expression in the CNS. Eur J Neurosci 20(2):467–473
41. Tanabe M, Nagatani Y, Saitoh K, Takasu K, Ono H (2009) Pharmacological assessments of nitric oxide synthase isoforms and downstream diversity of NO signaling in the maintenance of thermal and mechanical hypersensitivity after peripheral nerve injury in mice. Neuropharmacology 56(3):702–708
42. Kim KM, Pae H-O, Zhung M, Ha H-Y, Ha YA, Chai K-Y, Cheong Y-K, Kim J-M et al (2008) Involvement of anti-inflammatory heme oxygenase-1 in the inhibitory effect of curcumin on the expression of pro-inflammatory inducible nitric oxide synthase in RAW264. 7 macrophages. Biomed Pharmacother 62(9):630–636
43. Motterlini R, Foresti R (2014) Heme oxygenase-1 as a target for drug discovery. Antioxid Redox Signal 20(11):1810–1826
44. Liang D, Li X, Lighthall G, Clark J (2003) Heme oxygenase type 2 modulates behavioral and molecular changes during chronic exposure to morphine. Neuroscience 121(4):999–1005